

New Gamma-Ray Contributions to Supersymmetric Dark Matter Annihilation

Torsten Bringmann*

SISSA/ISAS and INFN, via Beirut 2 - 4, I - 34013 Trieste, Italy

Lars Bergström† and Joakim Edsjö‡

Department of Physics, Stockholm University, AlbaNova University Center, SE - 106 91 Stockholm, Sweden

(Dated: October 16, 2007)

We compute the electromagnetic radiative corrections to all leading annihilation processes which may occur in the Galactic dark matter halo, for dark matter in the framework of supersymmetric extensions of the Standard Model (MSSM and mSUGRA), and present the results of scans over the parameter space that is consistent with present observational bounds on the dark matter density of the Universe. Although these processes have previously been considered in some special cases by various authors, our new general analysis shows novel interesting results with large corrections that may be of importance, e.g., for searches at the soon to be launched GLAST gamma-ray space telescope. In particular, it is pointed out that regions of parameter space where there is a near degeneracy between the dark matter neutralino and the tau sleptons, radiative corrections may boost the gamma-ray yield by up to three or four orders of magnitude, even for neutralino masses considerably below the TeV scale, and will enhance the very characteristic signature of dark matter annihilations, namely a sharp step at the mass of the dark matter particle. Since this is a particularly interesting region for more constrained mSUGRA models of supersymmetry, we use an extensive scan over this parameter space to verify the significance of our findings. We also re-visit the direct annihilation of neutralinos into photons and point out that, for a considerable part of the parameter space, internal bremsstrahlung is more important for indirect dark matter searches than line signals.

PACS numbers: 13.40.Ks, 95.35.+d, 11.30.Pb, 98.70.Rz

I. INTRODUCTION

In view of the consensus that has become even stronger the last few years of the existence of a sizeable dark matter contribution to the total cosmological energy density, searches for experimental signatures that may determine the nature of the cosmological dark matter are becoming ever more important. The present estimates [1] give the fraction of the critical density of cold dark matter particles as $\Omega_{CDM}h^2 \sim 0.105 \pm 0.013$, where the Hubble parameter (scaled in units of 100 km/s Mpc⁻¹) is $h \sim 0.70 \pm 0.02$. Also, on the scales of galaxies and smaller, a number of methods including measurements of rotation curves as well as gravitational lensing agree well with the predictions from N-body calculations of gravitational clustering in cold dark matter cosmologies (see e.g. [2]).

The methods of detection of dark matter (for reviews, see [3]) can be divided into *accelerator* production and detection of missing energy (especially at the LHC at CERN, which will start operating some time in 2008), *direct detection* (of dark matter particles impinging on a terrestrial detector, with recent impressive upper limits reported by [4]), or *indirect detection* of particles generated by the annihilation of dark matter particles in the Galactic halo or in the Sun/Earth. All these methods are

indeed complementary – it is probable that a signal from more than one type of experiment will be needed to fully identify the particle making up the dark matter. The field is just entering very interesting times, with the LHC soon starting and new detectors of liquid noble gases being developed for direct detection. For indirect detection, the satellite PAMELA [5] was launched a year ago and will soon reveal its first sets of data for positron and antiproton yields in the cosmic rays [6]. AMANDA [7] at the South Pole that has searched for detection of neutrinos from the centre of the Earth or the Sun [8], will soon give way to the much larger detector IceCUBE [9], and for gamma-rays coming from annihilations of dark matter particles in the halo [10] the space satellite GLAST [11], to be launched in 2008, will open up a new window to the high-energy universe, for energies from below a GeV to about 300 GeV.

One problem with all these discovery methods is that the signal searched for may be quite weak, with much larger backgrounds in many cases. For indirect detection through gamma-rays, the situation may in principle be better, due to (i) the direct propagation from the region of production, without significant absorption or scattering; (ii) the dependence of the annihilation rate on the square of the dark matter density which may give "hot spots" near density concentrations as those predicted by N-body simulations; (iii) possible characteristic features like gamma-ray lines or steps, given by the fact that no more energy than m_χ per particle can be released in the annihilation of two non-relativistic dark matter particles (we denote the dark matter particle by χ).

As an example, it was recently shown [12] that in mod-

*Electronic address: bringman@sisssa.it

†Electronic address: lbe@physto.se

‡Electronic address: edsjo@physto.se

els of an extended Higgs sector, the line signal from the two-body final states $\gamma\gamma$ and $Z\gamma$ could give a spectacular signature in the gamma-ray spectrum between 40 and 80 GeV. On the other hand, in models of universal extra dimensions (UED) [13] or in the theoretically perhaps most favoured, supersymmetric, models of dark matter the line feature is in general not very prominent, except in some particular regions of the large parameter space. However, it was early realised that there could be other important spectral features [14], and recently it has been shown that internal bremsstrahlung (IB) from produced charged particles in the annihilations could yield a detectable "bump" near the highest energy for heavy gauginos or Higgsinos annihilating into W boson pairs, such as expected in split supersymmetry models [15]. In [16], it was furthermore pointed out that IB often can be estimated by simple, universal formulas and often gives rise to a very prominent step in the spectrum at photon energies of $E_\gamma = m_\chi$ (such as in UED models [17]).

Encouraged by these partial results, we have performed a detailed analysis of the importance of IB in the minimal supersymmetric extension to the standard model (MSSM). We have therefore calculated the IB contributions for all two-particle charged final states from general neutralino annihilations. Besides confirming the mentioned partial results for the universal radiative corrections, in particular those relating to soft and collinear bremsstrahlung, we also point out interesting cases of model-dependent "virtual" bremsstrahlung (i.e. photons emitted from charged virtual particles), see Fig. 1. We confirm the suspicion expressed already in [14] that this type of emission may circumvent the chiral suppression, i.e., the annihilation rate being proportional to m_f^2 for annihilation into a fermion pair from an S -wave initial state, as is the case in lowest order for non-relativistic dark matter Majorana particles in the Galactic halo (see also [18]). Since this enhancement mechanism is most prominent in cases where the neutralino is close to degenerate with charged sleptons, it is of special importance in the so-called stau coannihilation region in models of minimal supergravity (mSUGRA, as implemented in [19]). We therefore run through an extensive scan over these models (based on [20]) and find, indeed, remarkable cases of enhancement of the gamma-ray rate in the stau coannihilation region, near the maximal possible photon energy $E_\gamma = m_\chi$.

We want to emphasize the fact that the radiative corrections to the main annihilation channels, here computed systematically for the first time, may turn out to be of utmost importance when fitting gamma-ray data, e.g. from GLAST, to supersymmetric dark matter templates. Over much of the parameter space we have scanned, these corrections give a large factor of enhancement over the naive estimates, especially at the observationally most interesting, highest energies. More importantly, they add a feature, the very sharp step at the dark matter mass, that would distinguish this signal from all other astrophysical background (or foreground) processes.

II. SUPERSYMMETRIC EXTENSIONS TO THE STANDARD MODEL

Although our calculated electromagnetic radiative corrections will be applicable to the annihilation of any Majorana dark matter WIMP (weakly interacting massive particle), we will present results for the arguably most plausible dark matter candidate; the lightest neutralino in the MSSM, which is a linear combination of the superpartners of the gauge and Higgs fields:

$$\chi \equiv \tilde{\chi}_1^0 = N_{11}\tilde{B} + N_{12}\tilde{W}^3 + N_{13}\tilde{H}_1^0 + N_{14}\tilde{H}_2^0. \quad (1)$$

We perform all numerical calculations using the DarkSUSY code (see [21] for our sign conventions and other details).

The parameter μ is as usual the Higgsino mass parameter, $\tan\beta$ is the ratio of vacuum expectation values of the two Higgs doublets, M_1 , M_2 and M_3 are the gaugino mass parameters, m_A is the neutral pseudoscalar Higgs mass. We are also using parameters m_0 , A_t and A_b , defined through the simplifying ansatz: $\mathbf{M}_Q = \mathbf{M}_U = \mathbf{M}_D = \mathbf{M}_E = \mathbf{M}_L = m_0\mathbf{1}$, $\mathbf{A}_U = \text{diag}(0, 0, A_t)$, $\mathbf{A}_D = \text{diag}(0, 0, A_b)$, $\mathbf{A}_E = \mathbf{0}$. Here \mathbf{A} are soft trilinear couplings and \mathbf{M} soft sfermion masses which in general are 3×3 matrices in generation space, but are thus simplified through our ansatz and encoded in m_0 , A_t and A_b . We do not allow for CP-violating phases other than the CKM phase of the standard model. As a natural further simplification, the grand unification condition for the gauge couplings, leading to $M_1 = \frac{5}{3}\tan^2\theta_w M_2 \approx \frac{1}{2}M_2$ is used. For the MSSM scans, we use FeynHiggsFast [22] for the Higgs boson masses and decay widths. For each model, we will denote with m_χ the mass of the lightest neutralino and with $Z_g \equiv |N_{11}|^2 + |N_{12}|^2$ the gaugino fraction.

As a more restricted, but in some sense more natural, set of parameters we use those that stem from demanding that the electroweak symmetry be spontaneously broken by electroweak radiative effects such as appears in minimal supergravity (mSUGRA) models [23]. Also here we use the implementation in DarkSUSY [21], which relies on the public code Isajet [19] for the solution of the renormalization group equations (RGE) and for the mass spectra. In these models, parameters are given at the grand unification scale, and are then (using the RGEs) let to run down to the electroweak scale. The range of models with correct symmetry breaking are usually displayed in the m_0 - $m_{1/2}$ plane, where m_0 and $m_{1/2}$ are the universal scalar and gaugino masses, respectively, at the grand unification scale. The additional parameters of mSUGRA models are $\tan\beta$ (as for the MSSM), A_0 (which is the common trilinear term at the grand unified scale) and the sign of μ ($|\mu|$ is determined from the other parameters).

Let us briefly mention those regions in the m_0 - $m_{1/2}$ plane that are important from a cosmological point of view, as they correspond to models with a relic density in accordance with the WMAP value: The *bulk region* which has low m_0 and $m_{1/2}$; the *funnel region*

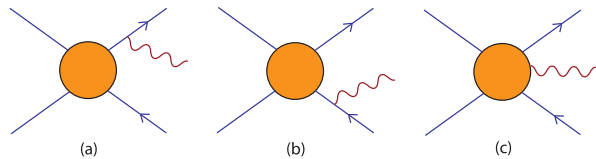


FIG. 1: Types of diagrams that contribute to the first order QED corrections to WIMP annihilations into a pair of charged particle final states. The leading contributions to diagrams (a) and (b) are universal, referred to as final state radiation (FSR), with a spectral distribution which only depends slightly on the final state particle spin and has been calculated, e.g., in [16]. Internal bremsstrahlung from virtual particles (or virtual internal bremsstrahlung, VIB) as in diagram (c), on the other hand, is strongly dependent on details of the short-distance physics such as helicity properties of the initial state and masses of intermediate particles.

$m_A \approx 2m_\chi$, where annihilations in the early universe are enhanced by the presence of the near-resonant pseudoscalar Higgs boson; the hyperbolic branch or *focus point region* where $m_0 \gg m_{1/2}$; the *stau coannihilation region* where $m_\chi \approx m_{\tilde{\tau}}$; and finally the *stop coannihilation region* (arising when $A_0 \neq 0$) where $m_\chi \approx m_{\tilde{t}}$. The stau coannihilation region has recently been noticed to have favourable properties for indirect detection rates in antiprotons and gamma-rays [24]. In this paper we will show that, in addition, there is a great enhancement of the high energy gamma-ray signature in this region.

III. INTERNAL BREMSSTRAHLUNG FROM WIMP ANNIHILATIONS

A. The general case

Whenever WIMPs annihilate into pairs of charged particles $X\bar{X}$, this process will with a finite probability automatically be accompanied by internal bremsstrahlung (IB), i.e. the emission of an additional photon in the final state (note that in contrast to ordinary, or external, bremsstrahlung no external electromagnetic field is required for the emission of the photon). As visualized in Fig. 1, one may distinguish between photons directly radiated from the external legs (*final state radiation*, FSR) and photons radiated from virtual charged particles (which we will refer to as *virtual internal bremsstrahlung*, VIB). So, to be more specific, *the IB photons will be the total contribution from both FSR and VIB photons.*

If the charged final states are relativistic, FSR diagrams are always dominated by photons emitted *collinearly* with X or \bar{X} . This is a purely kinematical effect and related to the fact that the propagator of the corresponding outgoing particle,

$$D(p) \propto ((k+p)^2 - m_X^2)^{-1}, \quad (2)$$

diverges in this situation. Here, k and p denote the momenta of the photon and the outgoing particle, respec-

tively. The resulting photon spectrum turns out to be of a universal form, almost independent of the underlying particle physics model [16, 17]. Defining the *photon multiplicity* as

$$\frac{dN_{X\bar{X}}}{dx} \equiv \frac{1}{\sigma_{\chi\chi \rightarrow X\bar{X}}} \frac{d\sigma_{\chi\chi \rightarrow X\bar{X}\gamma}}{dx}, \quad (3)$$

where $x \equiv 2E_\gamma/\sqrt{s} = E_\gamma/m_\chi$ and s is the center-of-mass energy, it is given by [16]:

$$\frac{dN_{X\bar{X}}}{dx} = \frac{\alpha Q_X^2}{\pi} \mathcal{F}_X(x) \log \left(\frac{s(1-x)}{m_X^2} \right). \quad (4)$$

Here, Q_X and m_X are the electric charge and mass of X ; the splitting function $\mathcal{F}(x)$ depends only on the spin of the final state particles and takes the form

$$\mathcal{F}_{\text{fermion}}(x) = \frac{1 + (1-x)^2}{x} \quad (5)$$

for fermions and

$$\mathcal{F}_{\text{boson}}(x) = \frac{1-x}{x} \quad (6)$$

for bosons. Due to the logarithmic enhancement that becomes apparent in Eq. (4), FSR photons are often the main source for IB. A prominent example where FSR in this universal form not only dominates IB but in fact the total gamma-ray spectrum from WIMP annihilations, is the case of Kaluza-Klein dark matter [17].

In general, one can single out two situations where photons emitted from virtual charged particles may give an even more important contribution to the total IB spectrum than FSR: i) the three-body final state $X\bar{X}\gamma$ satisfies a symmetry of the initial state that cannot be satisfied by the two-body final state $X\bar{X}$ or ii) X is a boson and the annihilation into $X\bar{X}$ is dominated by t -channel diagrams. To understand that the first case only leads to an enhancement of VIB, and not of FSR, we recall that the latter is dominated by collinear photons, i.e. the (virtual) final state particles are almost on mass-shell; the two- and three-body final states are thus bound to the same symmetry constraints. The enhancement of the annihilation rate in the second case follows from a closer inspection of the t -channel propagator. For non-relativistic WIMPs, it takes the form

$$D_t(p) \propto ((l-p)^2 - m_{\tilde{X}}^2)^{-1} \approx \left(m_\chi^2 - m_{\tilde{X}}^2 + m_X^2 + 2m_\chi E_X \right)^{-1}, \quad (7)$$

where l is the momentum of one of the ingoing WIMPs and \tilde{X} denotes the particle that is exchanged in the t -channel. If χ and \tilde{X} are almost degenerate in mass, one thus finds an enhancement for small E_X which – for kinematical reasons – corresponds to large photon energies E_γ . Note that this enhancement is less efficient for fermions since the infrared external spinor leg would result in a further suppression factor. In both cases, and in

contrast to the situation for FSR, the resulting spectrum is highly model-dependent. Prominent examples where VIB dominates over FSR as a consequence of these two special situations are neutralino annihilations into leptons [14] and charged gauge bosons [15], respectively, to which we will shortly return.

B. The neutralino case

The relevant final states of neutralino annihilations are W^+W^- , $W^\pm H^\mp$, H^+H^- and $f\bar{f}$; full analytical expressions for the corresponding rates can be found, e.g., in [3]. The inclusion of an additional photon in the final state is straight-forward, though tedious. Here, we are interested in the annihilation of neutralinos today, so we work in the limit of vanishing neutralino velocity – which greatly simplifies the calculation and the form of the analytical expressions. Our fully analytical results for arbitrary neutralino compositions agree with the special situations considered before, i.e. pure Higgsino or Wino annihilation into W^+W^- [15] and photino annihilation into $f\bar{f}$ in the limit of vanishing m_f [14].

Let us first note that for neutralino annihilations, in contrast to the situation for Kaluza-Klein dark matter, we cannot in general expect very large contributions from FSR (from external legs). This is because the lightest charged final states, for which the logarithmic enhancement shown in Eq. (4) would be most effective, are fermionic – but the annihilation rate of neutralinos into light fermions is strongly suppressed by a factor m_f^2/m_χ^2 due to the helicity properties of a pair of Majorana fermions in the limit of very small relative velocity [25]. On the other hand, as we will demonstrate now, all the possible final states for neutralino annihilations have the potential of showing considerable VIB contributions.

For large neutralino masses and charginos almost degenerate with the neutralino, for example, the W^+W^- and $W^\pm H^\mp$ final states fall into the second of the categories discussed in the previous subsection. In this limit, the photon multiplicity for W^+W^- final states is well approximated by [15]:

$$\begin{aligned} \frac{dN_{W^+W^-}}{dx} \simeq & \frac{\alpha_{\text{em}}}{\pi} \left[\frac{4(1-x+x^2)^2 \log(2/\epsilon)}{(1-x)x} \right. \\ & - \frac{2(4-12x+19x^2-22x^3+20x^4-10x^5+2x^6)}{(2-x)^2(1-x)x} \\ & \left. + \frac{2(8-24x+42x^2-37x^3+16x^4-3x^5)\log(1-x)}{(2-x)^3(1-x)x} \right] \end{aligned} \quad (8)$$

where $\epsilon \equiv m_W/m_\chi$. As demonstrated in the next section, the most significant IB contributions from final states with charged gauge bosons to the total annihilation spectrum are, in fact, of this form. The full analytical expressions for $dN_{W^+W^-}/dx$ and $dN_{W^\pm H^\mp}/dx$ are rather

lengthy and we will therefore not explicitly state them here, but we of course use them in our calculations.

As mentioned before, the annihilation into light fermions is helicity suppressed; for large photon energies, however, fermion final states containing an additional photon, $f\bar{f}\gamma$, are not subject to such a suppression. While our full analytical expressions are again rather lengthy, they simplify considerably in the limit of $m_f \rightarrow 0$. In this regime, we recover the expression found in [14], which includes a large enhancement factor m_χ^2/m_f^2 due to the lifted helicity suppression, and another large enhancement that is expected for sfermions degenerate with the neutralino.

Charged Higgs pairs H^+H^- , finally, provide yet another interesting example of the second category discussed in the previous subsection: In the limit $v \rightarrow 0$, this final state is not allowed because of CP conservation. The annihilation into $H^+H^-\gamma$, on the other hand, is possible. However, since charged Higgs bosons in most models have considerably larger masses than gauge bosons the enhancement mechanism described in the previous subsection is not as efficient as in the latter case. These final states are thus expected to be of less importance in our context.

In the last part of this section, let us briefly describe how we implemented IB from the various possible final states of neutralino annihilations in DarkSUSY. The total gamma-ray spectrum is given by

$$\frac{dN_{\gamma,\text{tot}}}{dx} = \sum_f B_f \left(\frac{dN_f^{\gamma,\text{sec}}}{dx} + \frac{dN_f^{\gamma,\text{IB}}}{dx} + \frac{dN_f^{\gamma,\text{line}}}{dx} \right), \quad (9)$$

where B_f denotes the branching ratio into the annihilation channel f . The last term in the above equation gives the contribution from the direct annihilation into photons, $\gamma\gamma$ or $Z\gamma$, which result in a sharp line feature [26]. The first term encodes the contribution from secondary photons, produced in the further decay and fragmentation of the annihilation products, mainly through the decay of neutral pions. This “standard” part of the total gamma-ray yield from dark matter annihilations shows a feature-less spectrum with a rather soft cutoff at $E_\gamma = m_\chi$. In DarkSUSY, these contributions are included by using the Monte Carlo code PYTHIA [27] to simulate the decay of a particle with mass $2m_\chi$ and user-specified branching ratios B_f . The resulting photon spectrum *does* include FSR (also from other particles in the decay cascade) but – since no details about the short-distance physics have been specified – of course not the full IB spectrum for neutralino annihilations and, in particular, not the contributions connected to VIB. In order not to count FSR photons twice, we thus adopt the following procedure: We calculate the full IB contribution as described before and then subtract the – analytically obtained – IB contribution from the decay of a hypothetical particle with mass $2m_\chi$ (which only contains the FSR part) from the PYTHIA simulation results. Hence, this procedure leaves us with corrected PYTHIA results with-

out FSR on the external legs and our analytical calculation of IB (including FSR and VIB) that we add to the corrected PYTHIA results. Note that this prescription is fully consistent since both parts are gauge-invariant separately. Let us conclude this section by showing in Fig. 2 four typical examples of mSUGRA models with particularly pronounced IB features. From top to bottom, they show situations in which IB from $t\bar{t}$, $\tau^+\tau^-$, all lepton and W^+W^- final states, respectively, dominates the total gamma-ray spectrum from DM annihilations.

IV. NUMERICAL RESULTS

We are now ready to apply the results in the previous section to a set of supersymmetric MSSM and mSUGRA models. For MSSM, we use a set of scans of the 7 parameters mentioned in Sec. II. These scans are fairly general and partly use the method of Markov Chain Monte Carlo models to focus on models that have the relic density in the WMAP preferred range. In total we have about 200 000 MSSM models that pass the WMAP relic density constraint and all accelerator constraints (checking experimental bounds on various masses and branching ratios, such as that of $b \rightarrow s\gamma$). For mSUGRA, we use the very large set of scans performed in Ref. [20] (also made with a Markov Chain Monte Carlo). This data set contains about 550 000 models that pass all the constraints.

Since the IB photons are most distinguished at higher energies (as seen in Fig. 2), we will integrate the flux above $0.6m_\chi$ and compare the flux in this energy range from the flux obtained from secondary photons (arising mainly from π^0 decays in quark jets). We will also compare it with the monochromatic gamma ray lines [26] that appear at loop-level.

In Fig. 3 we show our combined result for both the MSSM and mSUGRA models. In the left panel we show how IB compares with the regular secondary photons from quark jets. We plot this in the $Z_g/(1-Z_g)$ vs m_χ plane where gauginos (binos and winos) are at the top, Higgsinos are at the bottom and mixed neutralinos are in the middle. In the right panel, we show how IB photons compare with the monochromatic lines. It can be clearly seen that in large parts of this plane, IB photons are the *dominating component*, outnumbering both secondary and monochromatic photons. Hence, this effect is very important to include when searching for gamma ray signatures from dark matter.

In Fig. 3 we looked at the ratio of IB to other gamma ray contributions, let's now turn to the absolute fluxes. We can write the flux observed at earth as

$$\Phi_\gamma(E, \Delta\Omega, \psi) = 9.35 \cdot 10^{-14} \frac{dS}{dE} \times \langle J(\psi) \rangle (\Delta\Omega) \text{ cm}^{-2} \text{ s}^{-1} \text{ sr}^{-1}. \quad (10)$$

where we have put all the particle physics into the quan-

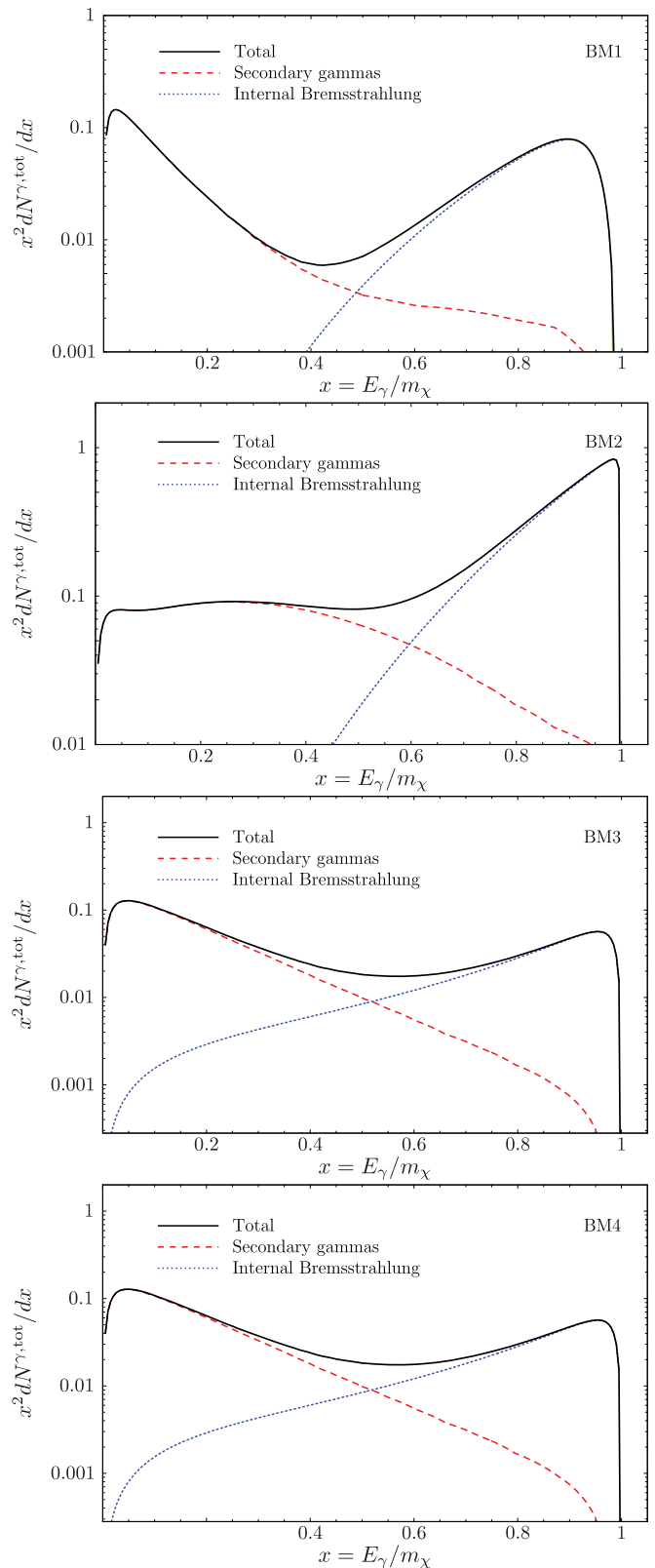


FIG. 2: From top to bottom, the gamma-ray spectra for the benchmark models defined in Tab. I is shown. The contributions from IB and secondary photons is indicated separately (in these figures, the line signal is not included).

Model	m_0 [GeV]	$m_{1/2}$ [GeV]	$\tan \beta$	A_0 [GeV]	$\text{sgn}(\mu)$	m_χ [GeV]	$Z_g/(1 - Z_g)$	Ωh^2	t -channel	\mathcal{S}	IB/sec.	IB/ $(\gamma\gamma + Z\gamma)$
BM1	3700	3060	5.65	$-1.39 \cdot 10^4$	-1	1396	$3.0 \cdot 10^4$	0.082	$\tilde{t}(1406)$	$8.1 \cdot 10^{-5}$	19.2	4.5
BM2	801	1046	30.2	$-3.04 \cdot 10^3$	-1	446.9	1611	0.110	$\tilde{\tau}(447.5)$	0.044	10.6	8.5
BM3	107.5	576.4	3.90	28.3	+1	233.3	220	0.084	$\tilde{\tau}(238.9)$	1.19	$2.3 \cdot 10^3$	5.0
BM4	$2.21 \cdot 10^4$	7792	24.1	17.7	+1	1926	$1.2 \cdot 10^{-4}$	0.11	$\tilde{\chi}_1^+(1996)$	0.012	10.8	2.1

TABLE I: Benchmark models that represent typical regions in the supersymmetric parameter space where IB becomes important. The “ t -channel” entry indicates the main contributing t -channel diagram, with the corresponding sparticle and its mass (all masses are given in GeV). $\mathcal{S} \equiv N_\gamma \frac{\langle \sigma v \rangle}{10^{-29} \text{ cm}^3 \text{ s}} \left(\frac{m_\chi}{100 \text{ GeV}} \right)^{-2}$ is the rescaled flux from IB alone and the last two columns give the ratio of the integrated flux, all above $0.6 m_\chi$, between the new IB contribution and secondary photons as well as the line signals. The main difference between BM2 and BM3 is that in the former neutralinos mainly annihilate into τ leptons, while in the latter mainly into t quarks. Also, for BM2 only the τ final states give an important contribution, while in the second case, even the other leptonic final states contribute considerably (due to near-degenerate slepton masses). For the BM4 model, the IB contribution from the W^+W^- state dominates.

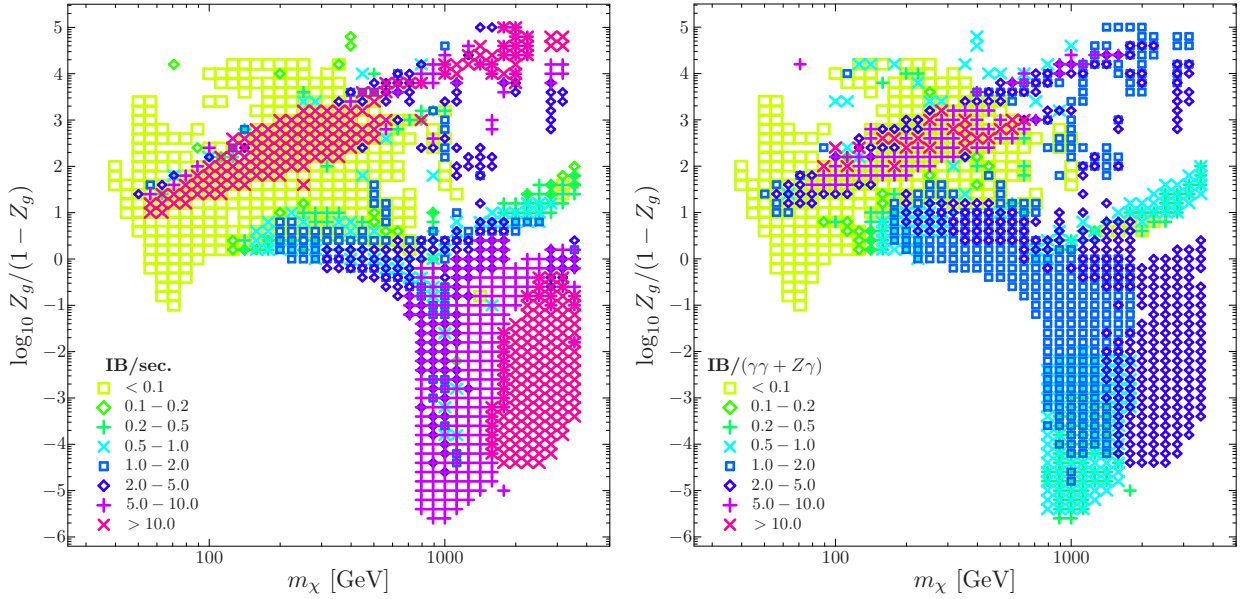


FIG. 3: Integrated internal bremsstrahlung flux from supersymmetric dark matter, above $0.6 m_\chi$, as compared to the “standard” continuum flux produced by secondary photons (left) and the flux from both line signals (right). As for the following figures (4 and 5), two symbols at the same location always indicate the whole interval between the values corresponding to these symbols. Every model considered here features a relic density as determined by WMAP and satisfies all current experimental bounds.

tity \mathcal{S} and the astrophysics into J . \mathcal{S} is given by

$$\left(\frac{d\mathcal{S}}{dE} \right)_{\text{IB } \gamma} = \left(\frac{100 \text{ GeV}}{m_\chi} \right)^2 \times \sum_f \left(\frac{v \sigma_f}{10^{-29} \text{ cm}^3 \text{ s}^{-1}} \right) \frac{dN_f^{\gamma, \text{IB}}}{dE} \quad (11)$$

where the sum is over all final states f . The astrophysical part (that depends on the chosen halo profile) is given by

$$\langle J(\psi) \rangle (\Delta\Omega) = \frac{1}{8.5 \text{ kpc}} \frac{1}{\Delta\Omega} \int_{\Delta\Omega} d\Omega' \times \int_{\text{line of sight}} dL \left(\frac{\rho(L, \psi')}{0.3 \text{ GeV/cm}^3} \right)^2. \quad (12)$$

For example, for a standard NFW [28] halo profile $\langle J \rangle \simeq 21$ averaged over $\Delta\Omega = 1$ sr towards the galactic centre. This value can be orders of magnitude larger though both for steeper profiles and/or for more concentrated observations towards the galactic centre (i.e. smaller $\Delta\Omega$ – as, e.g., for Air Cherenkov Telescopes). The effect of specific halo profiles and a more detailed analysis of the absolute fluxes with respect to the astrophysical background will be left for future work [29]. We will here focus on the particle physics factor \mathcal{S} .

In Fig. 4 we show the quantity \mathcal{S} , which is $d\mathcal{S}/dE$ integrated above $0.6 m_\chi$. In the left panel, we show the yields \mathcal{S} for the IB contribution, in the middle for monochromatic $\gamma\gamma$ and on the right for $Z\gamma$. In the regions where the IB contribution was the largest in Fig. 3, we typically have lower absolute yields. However, there are very

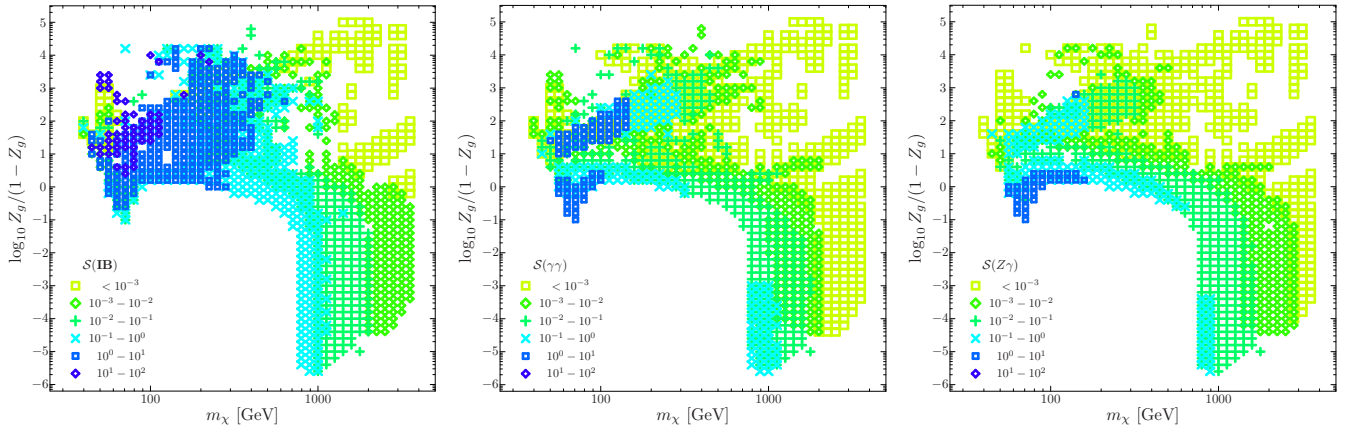


FIG. 4: The observationally relevant quantity $S \equiv N_\gamma \frac{\langle \sigma v \rangle}{10^{-29} \text{ cm}^3 \text{ s}} \left(\frac{m_\chi}{100 \text{ GeV}} \right)^{-2}$ for IB (left panel) and the line signals (middle and right panel). See text for more details.

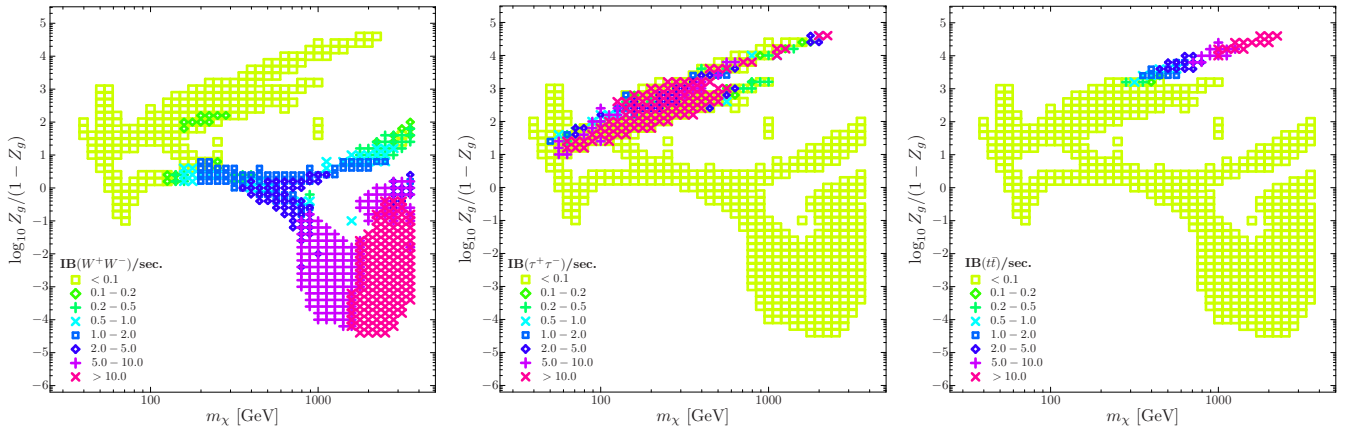


FIG. 5: As in the left panel of Fig. 3, but now for the individual contributions from various final states of neutralino annihilations in mSUGRA models. IB from light leptons covers a very similar region of the plotted parameter space as that from τ leptons. All (other) final states not shown here give always IB fluxes less than 10% of the flux from secondary photons.

pronounced regions, especially at small and intermediate masses, where the IB yields are very high even in absolute terms. We also note that, for neutralino masses in the TeV range, we expect a sizeable increase of the annihilation rate due to non-perturbative effects related to long-distance forces between the annihilating particles [30]. These effects have not been taken into account here and would result in a considerable enhancement (by a similar factor) of the quantity S for both line signals and IB.

In Fig. 5 we focus on the mSUGRA case and show the contribution relative to the secondary yield of gamma rays for various final states separately. In the left panel, we show the IB yield from the W^+W^- channel, in the middle from the $\tau^+\tau^-$ channel and in the right from the $t\bar{t}$ channel. Large IB contributions for the W^+W^- channel occur when a chargino is almost degenerate with the neutralino, as is the case for the focus point region. The large yields from the $\ell^+\ell^-$ and $t\bar{t}$ channels, on the other hand, occur when there is a strong degeneracy with the

lightest $\tilde{\ell}$ and \tilde{t} respectively. These latter cases occur in the phenomenologically important $\tilde{\tau}$ and \tilde{t} coannihilation regions: in these regimes, coannihilations with $\tilde{\tau}$ and \tilde{t} , respectively are needed to push the relic density down into the WMAP preferred region. Hence, we have a strong mass degeneracy between $\tilde{\chi}$ and $\tilde{\tau}/\tilde{t}$ which forces the IB contribution to the gamma yields to be strong.

As for the other possible final states, we note that the corresponding IB contributions never exceed 10% of the secondary photon flux; these channels are subdominant also for the MSSM models contained in our scan. In fact, from our discussion in the previous section, this is somewhat expected: Charged Higgs bosons, for example, are always heavier than charged gauged bosons, so multi-TeV neutralino masses would be needed for sufficiently large annihilation rates into $W^\pm H^\mp \gamma$ or $H^+ H^- \gamma$ (recalling that the annihilation rate in these cases is enhanced for relativistic final states). IB from light quarks is suppressed by the mass difference between the neutralino and the corresponding squark (as compared to the small

mass difference that can be achieved in the stop coannihilation region); down-type quarks, finally, receive a further suppression due to their smaller electric charge.

The main results of our paper may be more easily grasped by looking at the effect of IB on a small number of benchmark models. Of course, for the mSUGRA case, it is known that the exact location in parameter space of such benchmarks depends very sensitively on details of the calculation (see e.g. [31]). We therefore define our own set in Table I, which is very similar to that used by [20] except that we also include one point in the focus point region (BM4). This set of benchmark models is calculated with ISAJET 7.69 [19] together with DarkSUSY (see [20] for details). Point BM1 is a model where A_0 has been chosen large and negative to make the stop almost degenerate with the neutralino. BM2 is a model where the stau is almost degenerate with the neutralino and in BM3 also the selectron and the smuon are degenerate with the neutralino. BM4, finally, is in the focus point region, i.e. where the lightest chargino is almost degenerate with the lightest neutralino. The main IB characteristics of these benchmark models are summarized in Table I.

V. SUMMARY AND CONCLUSIONS

As can be seen already from our benchmark points in Table I, and in more detail from the scatter plots in Fig. 3, the internal bremsstrahlung effects computed in this work can be very significant, changing sometimes by more than an order of magnitude the lowest-order prediction for the high-energy gamma-ray signal from neutralino dark matter annihilation. Although some of these enhancements have been found before [14, 15, 16], this is the first time the first-order radiative corrections have been computed systematically, for all relevant final states in supersymmetric dark matter models. The resulting enhancements of the expected fluxes are surprisingly large over significant regions in the parameter space of MSSM, including the more constrained mSUGRA models. Despite the fact that some large corrections apply to absolute rates that are too small to be of practical interest, Fig. 4 shows that the quantity \mathcal{S} , which is directly proportional to the expected signal in gamma-ray detection experiments, also is significant for the internal bremsstrahlung contribution in large regions of parameter space. For $m_\chi < 300$ GeV, for example, values of \mathcal{S}_{IB} greater than 0.1 are generic, and for masses below 100 GeV, values of 1 or higher are common, which in

very many cases is higher than the corresponding values for the line signals $\gamma\gamma$ and $Z\gamma$.

We note that (as anticipated in [14]) helicity suppression and also CP selection rules of certain final states may be circumvented by emitting a photon; this is for example the origin of the very substantial enhancements of the signal obtained in the stau annihilation region in mSUGRA models. In this situation, the probability of emitting gamma rays vanishes at zero photon energy but increases rapidly at high energy (see Fig. 2b and 2c), which gives a photon “bump” at $E_\gamma \approx m_\chi$.

Of course, the line signals, in particular $\gamma\gamma$, have the virtue of being at the highest possible energy, so in order to make a more accurate comparison between these and the IB signal computed here, one would have to model also the expected spectral shape of possible astrophysical gamma-ray backgrounds and the energy resolution of the detector. This is left for future work [29]. We note, however, that in general also the new contributions have a characteristic signature, (*cf.* Fig. 2) which can hardly be mimicked by any known astrophysical gamma-ray source. In fact, in some cases these spectra could even be used by future experiments to distinguish between different dark matter candidates (note that, e.g., the distinction between Kaluza-Klein dark matter and a neutralino in the focus point region like our BM4 point would be possible already with the energy resolution of present Air Cherenkov Telescopes [32]).

To conclude, we have shown that the commonly neglected first-order radiative corrections to neutralino dark matter annihilation should definitely be taken into account when predicting rates for gamma-ray telescopes. In particular, the soon to be launched GLAST space telescope [11] will have an enhanced possibility over what has previously been assumed to detect radiation from supersymmetric dark matter annihilation. The routines needed to compute these new processes will be included in the next release of the DarkSUSY package [21, 33].

Acknowledgments

We wish to thank Piero Ullio, Maxim Perelstein, Michael Gustafsson and Martin Eriksson for useful discussions. L.B. and J.E. acknowledge support from the Swedish Research Council (VR). We are grateful to E.A. Baltz for letting us use his extensive data base of mSUGRA models.

-
- [1] D. N. Spergel *et al.* [WMAP Collaboration], *Astrophys. J. Suppl.* **170**, 377 (2007) [arXiv:astro-ph/0603449].
 - [2] J. Diemand, M. Kuhlen and P. Madau, *Astrophys. J.* **657**, 262 (2007) [arXiv:astro-ph/0611370].
 - [3] G. Jungman, M. Kamionkowski and K. Griest, *Phys. Rept.* **267**, 195 (1996) [arXiv:hep-ph/9506380];

- L. Bergström, *Rept. Prog. Phys.* **63**, 793 (2000) [arXiv:hep-ph/0002126]; G. Bertone, D. Hooper and J. Silk, *Phys. Rept.* **405**, 279 (2005) [hep-ph/0404175].
- [4] D. S. Akerib *et al.* [CDMS Collaboration], *Phys. Rev. Lett.* **96**, 011302 (2006) [arXiv:astro-ph/0509259]; J. Angile *et al.* [XENON Collaboration], arXiv:0706.0039

- [astro-ph].
- [5] P. Picozza *et al.*, *Astropart. Phys.* **27**, 296 (2007) [arXiv:astro-ph/0608697].
 - [6] J. Silk and M. Srednicki, *Phys. Rev. Lett.* **53**, 624 (1984); T. Bringmann and P. Salati, *Phys. Rev. D* **75**, 083006 (2007) [arXiv:astro-ph/0612514].
 - [7] A. Achterberg *et al.* [AMANDA Collaboration], *Astropart. Phys.* **26**, 129 (2006).
 - [8] G. Steigman *et al.*, *Astron. J.* **83**, 1050 (1978); W. H. Press and D. N. Spergel, *Astrophys. J.* **296**, 679 (1985); J. Silk, K. A. Olive and M. Srednicki, *Phys. Rev. Lett.* **55**, 257 (1985).
 - [9] S. Hundertmark [IceCube Collaboration], *Phys. Scripta* **T127**, 103 (2006).
 - [10] M. Srednicki, S. Theisen and J. Silk, *Phys. Rev. Lett.* **56**, 263 (1986) [Erratum-ibid. **56**, 1883 (1986)]; H. U. Bengtsson, P. Salati and J. Silk, *Nucl. Phys. B* **346**, 129 (1990); L. Bergström and H. Snellman, *Phys. Rev. D* **37**, 3737 (1988).
 - [11] N. Gehrels and P. Michelson [GLAST Collaboration], *Astropart. Phys.* **11**, 277 (1999).
 - [12] M. Gustafsson, E. Lundström, L. Bergström and J. Edsjö, *Phys. Rev. Lett.* **99**, 041301 (2007) [arXiv:astro-ph/0703512].
 - [13] L. Bergström, T. Bringmann, M. Eriksson and M. Gustafsson, *JCAP* **0504**, 004 (2005) [arXiv:hep-ph/0412001].
 - [14] L. Bergström, *Phys. Lett. B* **225**, 372 (1989).
 - [15] L. Bergström, T. Bringmann, M. Eriksson and M. Gustafsson, *Phys. Rev. Lett.* **95**, 241301 (2005) [arXiv:hep-ph/0507229].
 - [16] A. Birkedal, K. T. Matchev, M. Perelstein and A. Spray, arXiv:hep-ph/0507194.
 - [17] L. Bergström, T. Bringmann, M. Eriksson and M. Gustafsson, *Phys. Rev. Lett.* **94**, 131301 (2005) [arXiv:astro-ph/0410359].
 - [18] E. A. Baltz and L. Bergström, *Phys. Rev. D* **67**, 043516 (2003) [arXiv:hep-ph/0211325].
 - [19] F. E. Paige, S. D. Protopopescu, H. Baer and X. Tata, arXiv:hep-ph/0312045; H. Baer, F. E. Paige, S. D. Protopopescu and X. Tata, arXiv:hep-ph/0001086; <http://www.phy.bnl.gov/~isajet>.
 - [20] E. A. Baltz, M. Battaglia, M. E. Peskin and T. Wizansky, *Phys. Rev. D* **74**, 103521 (2006) [arXiv:hep-ph/0602187].
 - [21] P. Gondolo, J. Edsjö, P. Ullio, L. Bergström, M. Schelke and E. A. Baltz, *JCAP* **0407**, 008 (2004) [arXiv:astro-ph/0406204].
 - [22] S. Heinemeyer, W. Hollik and G. Weiglein, arXiv:hep-ph/0002213; *Phys. Rev. D* **58**, 091701 (1998) [arXiv:hep-ph/9803277]; *Eur. Phys. J. C* **9**, 343 (1999) [arXiv:hep-ph/9812472]; *Phys. Lett. B* **455**, 179 (1999) [arXiv:hep-ph/9903404].
 - [23] A. Chamseddine, R. Arnowitt and P. Nath, *Phys. Rev. Lett.* **49** (1982) 970; R. Barbieri, S. Ferrara and C. Savoy, *Phys. Lett.* **B119** (1982) 343; N. Ohta, *Prog. Theor. Phys.* **70** (1983) 542; L. J. Hall, J. Lykken and S. Weinberg, *Phys. Rev.* **D27** (1983) 2359; a review, see H. P. Nilles, *Phys. Rep.* **110** (1984) 1; J. L. Feng and T. Moroi, *Phys. Rev.* **D61** (2000) 095004; J. L. Feng, K. T. Matchev and T. Moroi, *Phys. Rev. Lett.* **84** (2000) 2322; J. L. Feng, K. T. Matchev and T. Moroi, *Phys. Rev.* **D61** (2000) 075005; J. L. Feng, K. T. Matchev and F. Wilczek, *Phys. Lett.* **B482** (2000) 388; H. Baer, C. Balazs, A. Belyaev, J. K. Mizukoshi, X. Tata and Y. Wang, *JHEP* **0207**, 050 (2002); J. R. Ellis, T. Falk, G. Ganiis and K. A. Olive, *Phys. Rev.* **D62**, 075010 (2000); J. R. Ellis, K. A. Olive, Y. Santoso and V. C. Spanos, *Phys. Lett.* **B565**, 176 (2003); J. Edsjö, M. Schelke, P. Ullio and P. Gondolo, *JCAP* **0304**, (2003) 001; H. Baer, A. Belyaev, T. Krupovnickas and X. Tata, *JHEP* **0402** (2004) 007.
 - [24] S. Profumo and A. Provenza, *JCAP* **0612**, 019 (2006) [arXiv:hep-ph/0609290].
 - [25] H. Goldberg, *Phys. Rev. Lett.* **50**, 1419 (1983).
 - [26] L. Bergström and P. Ullio, *Nucl. Phys. B* **504**, 27 (1997) [hep-ph/9706232]; P. Ullio and L. Bergström, *Phys. Rev.* **D57** (1998) 1962 [arXiv: hep-ph/9707333]; L. Bergström, P. Ullio and J. H. Buckley, *Astropart. Phys.* **9**, 137 (1998) [astro-ph/9712318].
 - [27] T. Sjöstrand, S. Mrenna and P. Skands, *JHEP* **0605**, 026 (2006) [arXiv:hep-ph/0603175].
 - [28] J. F. Navarro, C. S. Frenk and S. D. M. White, *Astrophys. J.* **490**, 493 (1997) [arXiv:astro-ph/9611107].
 - [29] T. Bringmann, M. Perelstein and P. Ullio, work in progress.
 - [30] J. Hisano, S. Matsumoto and M. M. Nojiri, *Phys. Rev. Lett.* **92**, 031303 (2004) [arXiv:hep-ph/0307216]; J. Hisano, S. Matsumoto, M. M. Nojiri and O. Saito, *Phys. Rev. D* **71**, 063528 (2005) [arXiv:hep-ph/0412403].
 - [31] M. Battaglia *et al.*, *Eur. Phys. J. C* **22**, 535 (2001) [arXiv:hep-ph/0106204].
 - [32] L. Bergström, T. Bringmann, M. Eriksson and M. Gustafsson, *AIP Conf. Proc.* **861**, 814 (2006) [arXiv:astro-ph/0609510].
 - [33] IB will be included in the next release of DarkSUSY [21]. If you need it earlier, please contact J. Edsjö (edsjo@physto.se).